review

Naturally occurring mutations in mice affecting lipid transport and metabolism

Karen Reue and Mark H. Doolittle

Lipid Research Laboratory, West Los Angeles VA Medical Center, and Department of Medicine, University of California-Los Angeles, Los Angeles, CA 90073

Abstract Naturally occurring mutations in the mouse provide a unique resource for identifying genes and characterizing proteins involved in lipid metabolism. Spontaneous mouse mutations have been described that affect various aspects of lipid metabolism, including cellular cholesterol homeostasis, fatty acid metabolism, serum lipoprotein levels, serum and tissue lipase activities, and lipid composition of tissues such as liver, nerve, kidney, and adrenal gland. Here we briefly describe the phenotypes and genetics of several mutants with blood and tissue lipid abnormalities, and then provide a more in-depth discussion of two mutations, fatty liver dystrophy (*fld*) and combined lipase deficiency (*cld*). Mice homozygous for the *fld* mutation exhibit fatty liver and hypertriglyceridemia during neonatal development, and a peripheral neuropathy that progresses throughout the lifetime of the animal. Combined lipase deficiency is characterized by a nearly complete absence of lipoprotein lipase and hepatic lipase activity resulting in neonatal lethality. Although the underlying genes for these two disorders have yet to be identified, candidates that have been implicated through the molecular and biochemical characterization of the mutants are discussed.—**Reue, K., and M. H. Doolittle.** Naturally occurring mutations in mice affecting lipid transport and metabolism. *J. Lipid Res.* 1996. **37:** 1387–1405.

Supplementary key words mouse mutations • lipoprotein lipase deficiency • lipase maturation • fatty liver • neuropathy

Naturally occurring mutations provide a unique tool for medical and biological research. In the field of lipid metabolism, the study of naturally occurring mutations and genetic variation in humans has contributed greatly to the identification of key proteins and to the delineation of key metabolic pathways. Notable among these are the elucidation of the low density lipoprotein receptor pathway, the role of lipoprotein lipase in triglyceride hydrolysis, the importance of apolipoprotein (apo) E in receptor binding and lipoprotein clearance, and the influence of apoA-I and high density lipoprotein levels on the development of atherosclerosis (reviewed in 1 and references therein).

In addition to human mutations, naturally occurring mutations in animal models provide a unique resource for identifying and characterizing genes involved in lipid metabolism (see references 2–6 for reviews). Among these models, the mouse has become firmly established as the most valuable mammalian model for genetic studies. For more than a thousand years, mouse fanciers around the world have bred mice for desirable or unique traits ranging from coat color to behavioral characteristics (7). Today, hundreds of inbred mouse strains exist, each serving as a potential source of genetic variation in traits or processes such as development, behavior, and disease susceptibility (8, 9). Furthermore, the process of inbreeding encourages the maintenance of spontaneously occurring mutations, particularly recessive mutations that might go undetected if sib-sib mating was not used.

Importantly for genetic studies, inbreeding also results in genetic homozygosity. This allows mapping of new genes and markers with relative ease, and also permits the collection of cumulative information about phenotype and genotype of any particular strain. To aid in the genetic dissection of interesting traits, tools such as congenic and recombinant inbred strains were developed as early as the 1940s and have been used for several decades (7). In recent years, however, gene mapping in the mouse has been revolutionized by the use of interspecific crosses between common laboratory mouse strains, *Mus musculus domesticus,* and related *Mus* species or subspecies (most commonly *Mus musculus castaneus* or *Mus spretus*) which have diverged evolutionarily for several million years (reviewed in references 10, 11). The

Abbreviations: apo, apolipoprotein; NP-C, Niemann-Pick disease Type C; SCAD, short-chain acyl-CoA dehydrogenase; PKD, polycystic kidney disease; LPL, lipoprotein lipase; HL, hepatic lipase; VLDL, very low density lipoproteins; FABP, fatty acid binding protein; NLSD, neutral lipid storage disorder; TAG, triacylglycerol; HDL, high density lipoproteins; ER, endoplasmic reticulum; cM, centimorgans; GlcNAc, N-acetylglucosamine; Man, mannose; Glc, glucose; PDI, protein disulfide isomerase; YAC, yeast artificial chromosome. For a list of locus names corresponding to mouse mutations, see Table 1.

TABLE 1. Naturally occurring mouse mutations affecting lipid metabolism

Name	Locus	Inheritance	Chromosome	Genetic Background	Phenotype	Reference[a]
Acyl-CoA dehydrogenase, short chain	*Acads*[b]	semi-dominant	5	BALB/cByJ	Short chain fatty acid oxidation defect; elevated excretion of fatty acid metabolites in urine; fasting induces fatty liver. Model for human short chain acyl-CoA dehydrogenase deficiency.	34, 35
Adrenocortical lipid depletion	*ald*	recessive	1	AKR/O	Depletion of cholesteryl esters from adrenal cortex at puberty; triglycerides and free cholesterol content normal.	41, 42
Combined lipase deficiency	*cld*	recessive	17	t-complex haplotype	Lipoprotein lipase and hepatic lipase deficiency; chylomicronemia; neonatal lethality.	51, 82
Congenital polycystic kidneys	*cpk*	recessive	12	C57BL/6J-pa	Elevated neutral and acidic glycolipids, decreased sulfolipid concentrations in kidney; apparent defect in sulfolipid synthesis; renal cysts. Model for human infantile polycystic kidney disease.	46, 48
Fatty liver dystrophy	*fld*	recessive	UN[c]	BALB/cByJ	Fatty liver, triglyceridemia, altered lipoprotein lipase and hepatic lipase expression in neonates; dyslipidemia corrects at age of weaning; peripheral neuropathy throughout adulthood.	52, 57
Foam-cell reticulosis	*fm*	recessive	UN	CBA/H	Accumulation of cholesterol and sphingomyelin in cells of lymphoid tissues and liver, but not brain; premature death at 6 months of age. Possible model for Niemann-Pick type C disease.	26
Juvenile visceral steatosis	*jvs*	recessive	11	C3H.OH	Fatty liver, hypoglycemia, hyperammonemia; reduced free and acyl-carnitine in serum; elevated urinary excretion of acylcarnitine. Resembles carnitine deficiency in humans.	36–38
Lysosomal cholesterol storage disorder	*lcsd*	recessive	UN	BALB/c (NCTR)	Foam cells in most visceral tissues with elevated cholesterol and sphingomyelin; defect in esterification of exogenous cholesterol. Possible model for Niemann-Pick type C disease.	25, 27
Neonatal intestinal lipidosis[d]	*Nil*	semi-dominant	7	A/Cam[e]	Accumulation of lipid in submucosa of small intestine; homozygotes die during gestation.	50
Edematous	*oed*	recessive	UN	phocomelic strain[e]	Plasma deficient in high-, low-, and very low-density lipoproteins, cholesterol, triglycerides, and phospholipids; elevated leukocytes; neonatal lethality.	39
Polycystic kidney disease	*pcy*	recessive	9	DBA/2FG	Abnormal phospholipid and fatty acid content in kidney; elevated serum phospholipid and cholesterol levels; renal cysts. Model for human adult-expressed polycystic kidney disease.	45, 47
Sphingomyelinosis	*spm*	recessive	18	C57BL/Ks[e]	Foam cells in liver and spleen, with elevated cellular cholesterol and sphingomyelin; defect in esterification of exogenous cholesterol; death by 3 months of age. Model for Niemann-Pick type C disease.	24, 28
Kit oncogene, viable dominant spotting	Kit^{Wv}[f]	semi-dominant	5	C57BL	Diminished lipoprotein lipase and hepatic lipase activity in post- heparin plasma; normal lipase activity in tissue; deficient in mast cells, and therefore, heparin.	53

[a]References cited are those describing the lipid abnormalities associated with each mutation.
[b]Formerly *bcd-1* (butyryl-CoA dehydrogenase).
[c]UN, unknown.
[d]Possibly extinct.
[e]Genetic background known to influence expression of mutant phenotype.
[f]Formerly W^v.

genetic divergence between these species allows detection of abundant DNA polymorphisms to facilitate gene mapping. Furthermore, interspecific crosses have provided the framework to allow systematic identification of genes contributing to polygenic traits and diseases (reviewed in reference 12). Finally, the ability to manipulate the mouse genome through the addition or inactivation of specific genes provides a method to observe the consequences of specific genetic alterations within the whole animal. For instance, several transgenic and gene knock-out mouse models have been developed to investigate the role of specific proteins in lipid metabolism and have been reviewed elsewhere (13–15). Despite the utility of these models, much can also be learned about lipid transport and metabolism from mouse mutations that have arisen spontaneously, and these mutations are the focus of this review.

More than 900 naturally occurring mouse mutations have been described that produce visible phenotypes affecting hair, skin, skeleton, growth and development, reproduction, blood components, internal organs, neurological and muscular systems, immune response, disease susceptibility, and behavior (9). A subset of about a dozen mutants that are known to exhibit blood or tissue lipid abnormalities is listed in **Table 1.** Mutations that specifically affect susceptibility to atherosclerosis or obesity are not included here as they have been reviewed previously (see references 15–20). The phenotypes of the mutations affecting lipid metabolism have been characterized to different degrees, some in depth over the course of many years and others only briefly at the time of their discovery. Most of these mutations are recessive, implying a loss of gene function, although a few act in a semidominant manner. As the genetic background on which the mutations occurred is known to influence expression of the phenotype in some cases (i.e., *Nil, spm,* and *oed*), the strain in which the mutation occurred is also noted in Table 1. While several of these mutations have been mapped to specific chromosomal regions, thus far only two of the mutant genes (*Acads* and *Kit*^{wv}) have been cloned (21, 22). We will briefly describe the phenotypes of mutants expressing blood and tissue lipid abnormalities listed in Table 1 and then provide a more in depth discussion of two of these mutants that are subjects of our current research, *fld* (fatty liver dystrophy) and *cld* (combined lipase deficiency).

Mutations affecting cellular cholesterol metabolism

The foam cell reticulosis (*fm*), lysosomal cholesterol storage disorder (*lcsd*), and sphingomyelinosis (*spm*) mutations are characterized by defects in cellular cholesterol metabolism and resemble the human disorder Niemann-Pick disease Type C (NP-C). NP-C is an autosomal recessive defect in cellular esterification of exogenous cholesterol, resulting in an accumulation of cholesterol within the lysosomes (23). Homozygous *spm* and *lcsd* mice are recognizable between 1 and 2 months of age by the development of a tremor, loss of coordination, and weight loss, followed by death at the age of 3 months (24, 25). Symptoms in *fm* mutants develop slightly later (3–4 months of age, death at 6 months) and involve weight loss and inactivity without the neuropathy seen in *spm* and *lcsd* mice (26). On some genetic backgrounds but not others, the *spm* mice exhibit hepatosplenomegaly, a classic symptom of NP-C, implying that the action of modifier genes may influence the phenotype.

The histopathology of the *fm, lcsd,* and *spm* mutants is very similar with an accumulation of lipid-filled foam cells in liver, spleen, and in some cases thymus and lymph nodes, but never in brain (26–28). The *spm* and *lcsd* mutants also exhibit a depletion of Purkinje cells and degeneration of the cerebellum, a characteristic feature of severe NP-C. Fibroblasts isolated from *lcsd* and *spm* mice, as well as from NP-C patients, exhibit defective esterification of exogenous cholesterol, including LDL cholesterol (23, 29, 30). Furthermore, in the case of the *lcsd* mutation, defects in acyl-CoA:cholesterol acyltransferase and in the transport of exogenous cholesterol to microsomes have been ruled out (29). Interestingly, in contrast to the defect in esterification of exogenously derived cholesterol, cellular synthesis of cholesteryl esters from mevalonic acid and squalene is normal (29). These findings all point to a disruption of a step in cholesterol esterification that occurs subsequent to delivery of cholesterol to microsomes.

In addition to increased cellular cholesterol concentration, *fm, lcsd,* and *spm* mutants display increased sphingomyelin content due to a reduction in sphingomyelinase activity. However, the sequence of the acid sphingomyelinase gene from *lcsd* and *spm* homozygotes is normal, indicating that the reduction in this enzyme activity is secondary to the primary defect in cholesterol transport (31). These findings distinguish the *lcsd* and *spm* mutations from Niemann-Pick type A, which results from mutation in the acid sphingomyelinase gene (23). Although no naturally occurring mutations have been described in the mouse sphingomyelinase gene, a mouse model of Niemann-Pick type A has been produced by targeted inactivation of this gene (32).

It has been suggested that the *spm* mutation represents the homologue of the gene underlying human NP-C, as the *spm* mutation maps to chromosome 18, syntenic with the position of NP-C on human chromosome 18 (30). Additional evidence that *spm* is a homologue of the NP-C gene comes from the demonstration

that normal cholesterol metabolism can be restored in *spm* fibroblasts by transfection with human chromosome 18 (33). As *lcsd* and *fm* have not been mapped, it is not yet possible to determine whether they represent loci distinct from *spm* or alternate mutant alleles of the *spm* locus.

Mutations affecting fatty acid metabolism

Spontaneous mouse mutations which may serve as models for human defects in fatty acid metabolism have also been identified. A mutation was detected in the structural gene (*Acads*) for the enzyme short-chain acyl-CoA dehydrogenase (SCAD), an enzyme required for complete β-oxidation of short-chain fatty acids (22). SCAD-deficient mice are not distinguishable from wild-type mice by physical appearance, but secrete large amounts of fatty acid metabolites in the urine (34, 35). In addition, when fasted for 18 h, the SCAD mice develop fatty liver as a result of increased reliance on the mobilization of fatty acids to the liver for oxidation; short-chain fatty acids that cannot be oxidized are esterified and stored in the form of triglycerides giving rise to the fatty liver. The SCAD mice may be useful as a model for investigating short-chain fatty acid metabolism, and as a model for the same rare disorder in humans. It should be noted, however, that the clinical severity of SCAD deficiency is less in mice than in humans. This has been attributed to the greater efficiency with which rodents eliminate short-chain fatty acid metabolites (34, 35).

The juvenile visceral steatosis (*jvs*) mutant mouse exhibits a phenotype similar to carnitine deficiency in humans (36). Carnitine is required for transport of long-chain fatty acids into the mitochondria for β-oxidation, and a deficiency results in impaired energy production and triglyceride accumulation in liver, skeletal muscle, and heart. Hallmark features of the *jvs* phenotype include retarded growth rate, fatty liver, hypoglycemia, and hyperammonemia, all of which may be present in human systemic carnitine deficiency. Levels of carnitine and acyl-carnitine are significantly reduced in serum, whereas urinary excretion of acylcarnitine is elevated. The hyperammonemia in *jvs/jvs* mice appears to result from reduced expression of urea cycle enzymes (37). Interestingly, administering carnitine to *jvs/jvs* mice restores urea cycle enzyme expression and activities to normal levels, but does not reduce hepatic lipid levels to normal (38). These studies indicate that carnitine deficiency, rather than hepatic lipid accumulation, directly influences urea cycle enzyme expression. The carnitine deficiency in *jvs/jvs* mice is associated with increased carnitine excretion and reduced rates of sodium-dependent carnitine uptake in kidney slices, suggesting that the primary defect lies in the reabsorption of carnitine in the kidney (39).

Mutants with blood and tissue lipid abnormalities in unidentified pathways

Several mouse mutants characterized by abnormal blood lipid concentrations or the accumulation of lipids in tissues have been described. Mice homozygous for the edematous mutation (*oed*), for example, exhibit an extreme blood lipid phenotype with deficiencies in high, low, and very low density lipoproteins, cholesterol, triglycerides, and phospholipids (40). It has been shown that the rate of syntheses of triglyceride, cholesteryl esters, and fatty acids are reduced in the liver. In addition to the lipid abnormalities, these mice have shiny brittle skin, a 3-fold elevation in leukocyte concentration, and die shortly after birth. It may be significant that this mutation occurred in a strain carrying phocomelia (*pc*), a neonatal lethal recessive mutation that affects skeletal development of the head and limbs and produces cleft palate (41). The underlying defect in *oed/oed* mouse has not been identified, nor has the mutation been mapped in the mouse genome.

Lipid depletion within the adrenal gland is the hallmark phenotype associated with the adrenocortical lipid depletion (*ald*) mutation. Homozygotes for the mutant allele exhibit spontaneous depletion of cholesteryl esters from the adrenal cortex coincident with the onset of puberty; free cholesterol and triglyceride levels in this tissue remain normal (42). However, the primary site of *ald* expression appears not to be the adrenal gland, as demonstrated by the normal lipid content of adrenal glands from mutant mice after transplantation into unaffected animals (43). Interestingly, the *Acact* gene that encodes acyl-CoA:cholesterol acyltransferase, the enzyme responsible for intracellular cholesterol esterification, has recently been localized on chromosome 1 near *ald* (44). This gene is an excellent candidate for *ald* and studies are underway to determine whether a mutation in *Acact* is responsible for the adrenal lipid depletion phenotype.

The polycystic kidney disease (*pcy*) and congenital polycystic kidneys (*cpk*) mutations affect lipid levels and composition in the kidney. As many as five independent loci have been associated with polycystic kidney disease (PKD) in the mouse, but thus far lipid abnormalities have been described only for *pcy* and *cpk* (45, 46). The phenotype conferred by the *pcy* mutation resembles human adult-expressed dominant PKD (although it is inherited as a recessive trait in mice), whereas that for *cpk* resembles human infantile recessive PKD (47, 48). Mice homozygous for the *pcy* mutation exhibit progressive renal enlargement and the development of cysts beginning at 8 weeks of age, as well as altered serum and

tissue lipid composition. Serum phospholipid and cholesterol levels are elevated (123% and 35%, respectively), as is the cholesterol/phospholipid ratio in kidney (45). The abnormal phospholipid and fatty acid composition in kidney may alter membrane fluidity and membrane functions such as receptor activation, signal transduction, and ion transport.

Mice homozygous for the *cpk* mutation are afflicted with a rapidly progressive disease, with renal cysts detectable at 10 days, and death occurring at 3 weeks (48). The kidneys exhibit a marked decrease in sulfotransferase activity, with a concomitant decrement in sulfolipid content (46). In addition, levels of neutral glycolipids and the acidic lipid ganglioside GM3 are elevated. Based on this model, it has been suggested that abnormal sphingolipid content may contribute to the proliferative and transport abnormalities associated with PKD (46). The *pcy* and *cpk* genes have been mapped to separate chromosomes and therefore are not allelic (47, 49); thus far, candidates have not been identified based on either genetic or biochemical data.

Another mutation affecting tissue lipid content is neonatal intestinal lipidosis (*Nil*). Unlike many of the mutations presented in Table 1, *Nil* displays a semidominant pattern of expression. As newborn mice begin to suckle, heterozygotes carrying one mutant allele exhibit a thickening of regions of the small intestinal wall and an accumulation of lipid in the submucosa (50). The lipid accumulation may persist until after weaning, and affected adults may also exhibit reduced fertility and viability. As with many of the lipid mutants, expression of the phenotype in heterozygotes depends on the genetic background. Homozygotes for the mutation are not viable and die during mid-gestation. The *Nil* mutation was mapped to chromosome 7, but unfortunately mice carrying the mutation are thought to be extinct making further studies impossible.

The combined lipase deficiency (*cld*), fatty liver dystrophy (*fld*), and viable dominant spotting (Kit^{wv}) mutations are each characterized by alterations in triglyceride metabolism, with extreme (*cld*), moderate (*fld*), or variable (Kit^{wv}) hypertriglyceridemia occurring as the newborn mice begin to suckle (51–53). Underlying the hypertriglyceridemia in all cases are deficiencies affecting lipoprotein lipase (LPL) and hepatic lipase (HL) activities. However, the biochemical defects associated with the three mutations appear to be quite different. For example, it has been established that mice carrying the W^v mutant allele of the *Kit* gene have greatly diminished LPL and HL activity in post-heparin plasma, but have normal activity in tissues (LPL in adipose and heart; HL in liver) (53). These mice lack mast cells, and it has been suggested that the resulting heparin deficiency may prevent normal attachment of the lipases to endothelial surfaces, thus impairing hydrolysis of lipoproteins in the circulation. Mice homozygous for the *fld* mutation also synthesize active lipases in the tissues, but exhibit abnormal developmental regulation of the expression levels. Thus, LPL mRNA and activity levels are dramatically reduced in white adipose tissue during neonatal development, but return to normal after weaning (52). In contrast to the *Kit* and *fld* mutants, the *cld* mutation results in the synthesis of inactive lipoprotein lipase and hepatic lipase molecules due to aberrant maturation within the endoplasmic reticulum. Our laboratories are seeking to uncover the underlying defect in the *fld* and *cld* mice. Our current understanding of the molecular, genetic, and biochemical bases of these two interesting mutations is discussed in detail below.

Fatty Liver Dystrophy Mutation

Fatty liver dystrophy (*fld*) is an autosomal recessive mutation that occurred spontaneously in a BALB/cByJ mouse breeding colony at the Jackson Laboratory in 1981 (54). At birth the mutant mice are indistinguishable from their littermates. However, after the first days of suckling, *fld/fld* animals become recognizable by the appearance of a swollen abdomen and enlarged pale liver which is visible through the skin. The mutant mice are smaller and mature more slowly than their unaffected littermates, with reduced coat growth apparent between 1–2 weeks of age (**Fig. 1**). Mutant mice eventually develop a sparse, ruffled coat of fur that contrasts with the normal sleek coat of wild-type mice. During the

Fig. 1. Ten-day-old *fld/fld* and wild-type littermates. Ten-day-old *fld/fld* mouse (front) next to a wild-type littermate. At this age, *fld/fld* animals have a body weight of only 50–60% that of their unaffected littermates, exhibit delayed hair growth, and enlarged abdomen due to hepatomegaly (not visible in photograph).

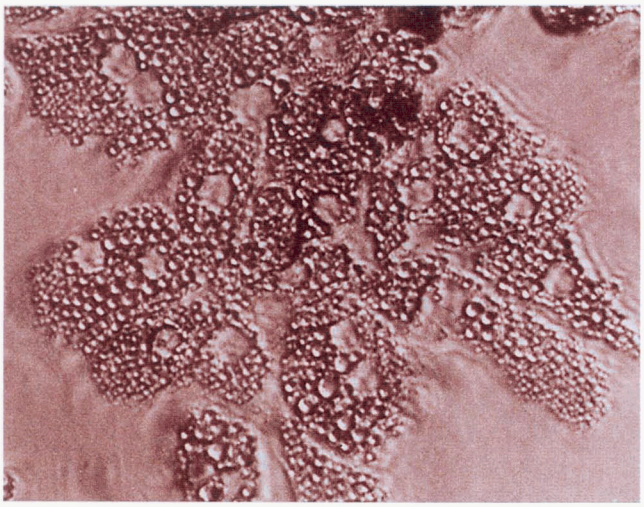

Fig. 2. Light micrograph of hepatocytes from 10-day-old *fld/fld* mouse. Hepatocytes were isolated by perfusion through the portal vein with collagenase (118). Released cells were washed extensively and plated onto collagen-coated dishes and grown in culture for 2 days. An accumulation of large intracellular droplets is apparent throughout the cytoplasm of hepatocytes when viewed under phase contrast optics. Nuclei appear as round spaces in the cytoplasm. Magnification is 400×.

transition from suckling to weaning (13–15 days of age), the liver spontaneously returns to normal size and color with no apparent permanent cellular pathology (52). Although it occurs at a time that coincides with weaning, resolution of the fatty liver does not appear to be determined by the change in diet (discussed in a later section).

At 2–3 weeks of age, a second feature of the *fld* phenotype becomes evident. The mice develop a generalized tremor and unsteady movements, particularly with the hind legs (55). The mutant mice also exhibit an unusual response to handling: when picked up by the tail, the animals clench their toes and clasp the rear legs together in contrast with the normal reflex to extend the legs outward. The neuropathy is associated with pathology in the peripheral, but not central, nervous system (described below), and unlike the fatty liver syndrome, progresses throughout the lifetime of the animal. Adult *fld/fld* mice also remain smaller than normal littermates with a 25–35% reduction in body weight (K. Reue, unpublished observations). A proportion of *fld/fld* mice typically die between 3–5 weeks of age, and those that survive to adulthood have a limited reproductive capacity. Males are infertile, although the reproductive organs appear normal; many females breed, although they begin to produce offspring at a later age than normal mice.

Aberrant triacylglycerol metabolism in neonatal fld/fld *mice.* The pale fatty liver in neonatal *fld/fld* mice is due to an accumulation of large lipid droplets within hepatocytes (see **Fig. 2**). In addition, hypertrophy is evident in these hepatocytes due to the large mass of intracellular lipid, thus resulting in the characteristic hepatomegaly. Hepatocytes isolated by perfusion of livers from 10-day-old *fld/fld* mice appear identical to those examined in situ, and can be maintained in culture for several days without loss of lipid from the cells (K. Reue and M. H. Doolittle, unpublished observations). Isolated hepatocytes exhibit additional hallmark features of the fatty liver, such as altered levels of apolipoprotein and lipase expression (see below). Analysis of the lipids from the fatty liver of 7–14 day old *fld/fld* mice revealed that triacylglycerol levels are elevated 6-fold, with a slight elevation in diacylglycerol, but no apparent changes in cholesterol, cholesteryl esters, or phospholipids (**Fig. 3**). An elevation in free fatty acid level is also evident in the fatty liver at 7 days of age. In contrast, at 30 days of age and older, hepatic lipids of *fld/fld* mice appear completely normal (Fig. 3).

Concomitant with the fatty liver, neonatal *fld/fld* mice exhibit hypertriglyceridemia (1000 mg/dl), elevated plasma fatty acid levels, and a complex array of tissue-specific alterations in the expression of several proteins involved in lipoprotein metabolism (52 and K. Reue, unpublished data). For example, in 7-day-old mutant

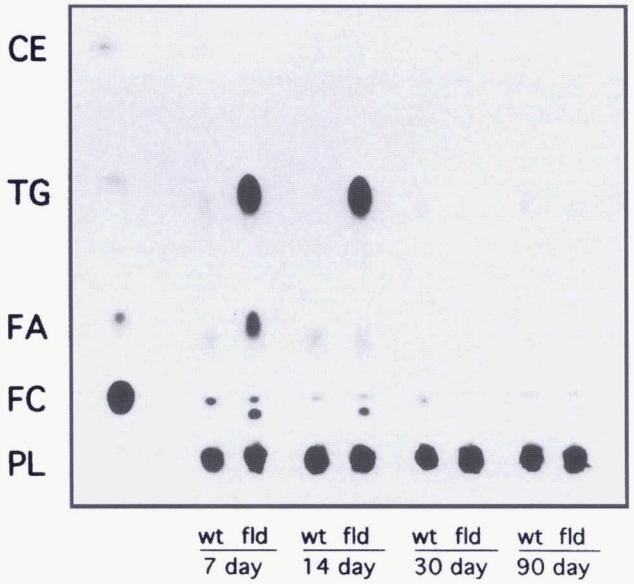

Fig. 3. Thin-layer chromatogram of neutral lipids from liver of *fld/fld* and wild-type mice. Lipids were extracted from liver homogenates of *fld/fld* and wild-type mice aged 7, 14, 30, and 90 days, and aliquots containing equivalent amounts of protein were applied to a silica gel plate. The chromatogram was developed in hexane–ethyl ether–acetic acid 80:20:1 and detected by charring in 3% cupric acetate/8% phosphoric acid. Lipid species were identified by comparison to standards, shown in the lane at far left: cholesteryl ester (CE), triacylglycerol (TG), fatty acid (FA), free cholesterol (FC), and phospholipid (PL). The species migrating directly below free cholesterol, which is visible in 7- and 14-day-old *fld/fld* liver, is diacylglycerol.

mice, LPL in white adipose tissue is reduced to approximately 5% of normal activity, whereas LPL activity is reduced only slightly in brown adipose tissue and heart. Although LPL expression in liver is not altered significantly, the liver-derived hepatic lipase activity is reduced to 20% of normal levels. In contrast, mRNA levels for apolipoproteins A-IV and C-II are significantly elevated in liver (100-fold and 6-fold, respectively), yet appear normal in intestine. A comparison of total protein expression patterns in the fatty liver of 5-day-old *fld/fld* mice and their wild-type littermates using quantitative two-dimensional gel electrophoresis revealed that approximately two dozen proteins exhibit altered expression, with the majority having increased expression in the fatty liver (56). Although most of the altered expression levels likely represent secondary effects of the underlying *fld* mutation, an identification of these proteins may provide insight into the biochemical defect and suggest candidates for the *fld* gene product.

The metabolic defect in triacylglycerol metabolism that leads to development of the fatty liver is not yet known. The activity of lysosomal acid triacylglycerol lipase, the enzyme responsible for hydrolysis of exogenous triacylglycerols entering the liver, appears normal in liver homogenates prepared from neonatal and adult *fld/fld* mice (K. Reue, unpublished data). Furthermore, the rate of hepatic triacylglycerol synthesis from radiolabeled fatty acids in 3-day-old *fld/fld* mice is not increased; instead, the proportion of label incorporated into phospholipid is increased (K. Reue, unpublished data). Thus, although it is likely that increased triacylglycerol synthesis occurs during formation of the fatty liver within the first post-natal day, it is not ongoing within the fatty liver throughout the neonatal period.

Preliminary studies suggest that the metabolism of fatty acids released from triacylglycerol hydrolysis may be impaired in the fatty liver, as the efficiency of palmitate oxidation is reduced in cultured hepatocytes from 10-day-old *fld/fld* mice (56). In line with these results is the observation that the ultrastructure of *fld/fld* mitochondria in electron micrographs appears ill-defined, with reduced definition of cristae (B. G. Slavin and K. Reue, unpublished data). However, it appears that isolated mitochondria from *fld/fld* liver exhibit normal oxidation rates raising the possibility that peroxisomal oxidation may be affected in the *fld/fld* cells (56). While an examination of the organic acids present in the fatty liver of *fld/fld* neonates via mass spectrometry–gas chromatography failed to reveal an accumulation of metabolites (K. Reue and L. Sweetman, unpublished data), characteristic of human fatty acid oxidation disorders, it should be noted that elimination of some fatty acid metabolites occurs with greater efficiency in mice than in humans (35). Further studies will be necessary to determine whether the reduced fatty acid oxidation in the fatty liver is a primary or secondary effect of the mutation, and to identify the underlying enzyme(s) involved. It should also be noted that the mutation in the short chain acyl-CoA dehydrogenase gene (*Acads*), which occurred in the same strain as the *fld* mutation and which prevents complete oxidation of short chain fatty acids (described earlier), is not present in *fld/fld* mice and thus does not contribute to the fatty liver phenotype (K. Reue and R. D. Cohen, unpublished data).

An intriguing feature of the neonatal *fld/fld* phenotype is the invariable correction of the fatty liver and hypertriglyceridemia (at 13–15 days of age) and of the aberrant lipase and apolipoprotein expression levels (by 28–34 days of age). Although the correction of the fatty liver coincides with a switch from triglyceride-rich mouse milk to low-fat, high-carbohydrate laboratory chow, the correction appears not to result directly from the change in diet. Evidence for this comes from the demonstration that a prolonged suckling period of 20 days does not perpetuate the hypertriglyceridemia or fatty liver, nor can feeding a high fat diet to adult *fld/fld* mice elicit a fatty liver (52). Based on these observations, it appears that the *fld* gene product is required to maintain lipid homeostasis during the neonatal period, but that induction of an additional protein or process at a particular stage of development may mask or compensate for the *fld* defect. One candidate for such a developmentally regulated process is the initiation of very low density lipoprotein (VLDL) secretion which occurs in rodent liver near the time of weaning (57). Thus, it is possible that the combination of a reduction in dietary fat and the initiation of VLDL secretion results in the correction of the fatty liver near the age of weaning.

Abnormal structure, protein and lipid content of peripheral nerve in fld/fld *mice.* The peripheral neuropathy becomes apparent at the end of the fatty liver period (2–3 weeks of age) and persists throughout the lifetime of *fld/fld* mice. Langner et al. (55) determined that the neuropathy is associated with abnormalities in peripheral nerve myelin structure including thin, poorly compacted myelin sheaths, ongoing myelin breakdown, and enlarged Schwann cell mitochondria. Coincident with the morphologic changes are greatly diminished levels of the major peripheral myelin protein P_0, and undetectable amounts of myelin protein P_2, which is expressed primarily in the cytosol of Schwann cells in peripheral nerve. Interestingly, mice lacking P_0 have been produced by gene targeting and exhibit some behavioral and pathological phenotypes seen in *fld/fld* mice. For example, P_0 knock-out mice develop a tremor with dragging or jerky movements of the rear legs, clasp the hindlimbs together when lifted by the tail, and exhibit

abnormal compaction and maintenance of peripheral nerve myelin sheaths (58). However, the P_0 knock-out mice also develop convulsions and additional behavioral abnormalities, and do not display the other manifestations of the *fld* mutation such as fatty liver, hypertriglyceridemia, or retarded growth.

Myelin protein P_2 is a member of the family of small cytoplasmic lipid binding proteins that includes fatty acid binding proteins (FABPs) in liver, intestine, and heart, as well as the adipocyte protein aP2 (59). The expression of other members of this family are moderately altered in *fld/fld* tissues, with a 2- to 3-fold reduction in steady state levels of liver FABP (55), and a 5-fold increase in aP2 mRNA levels in epididymal adipose from 9-day-old *fld/fld* mice (K. Reue and R. D. Cohen, unpublished data). As myelin P_2 and other members of the FABP family appear to have arisen from a common ancestral gene (59), it is possible that common regulatory sequences are shared among the genes as well. Thus, altered expression levels of several members of the FABP family in the *fld/fld* mouse could potentially result from change in the activity of a shared regulatory protein.

In contrast to the diminished levels of myelin proteins P_0 and P_2, *fld/fld* nerve exhibits elevated levels of apolipoprotein E and GAP-43 (55), proteins that are induced during nerve development or in response to nerve injury. The lipid composition of *fld/fld* peripheral nerve myelin is also abnormal, although lipid composition in the brain appears normal. As determined by high performance thin-layer chromatography, sciatic nerve from *fld/fld* mice shows an age-dependent progressive decrease in levels of phospholipids and glycosphingolipids, and an elevation in cholesteryl ester levels (55). Overall, the protein and lipid profile of *fld/fld* peripheral nerve resembles that of immature nerve and indicates an ongoing regenerative response.

Several other mouse mutations that are associated with pathological changes in the peripheral nerve have been described (reviewed in reference 55). Of these other mutants, the trembler (*Tr*) mutation is characterized by an abnormal nerve lipid profile which is most similar to that seen in the *fld/fld* mouse, including age-dependent decreases in phospholipids and glycosphingolipids, and elevated cholesteryl esters. However, the trembler gene has been identified as that encoding peripheral myelin protein 22 (60), and linkage to the *fld* locus has been excluded (55). Furthermore, neither the trembler mouse nor other mutants with peripheral nerve defects exhibit any aspect of the fatty liver phenotype that occurs in neonatal *fld/fld* mice.

Relationship of the fld *mutation to human disease.* Several human diseases are known that are characterized by both neuropathy and aberrant fatty acid metabolism. These include defects in peroxisome or mitochondrial function such as Refsum's disease, adrenomyeloneuropathy, and acetoacetyl-CoA thiolase deficiency (reviewed in 61, 62). However, the *fld* phenotype does not faithfully mirror the overall clinical and biochemical features of any of these human disorders. The *fld* phenotype does share several features in common with human neutral lipid storage disease (NLSD), also known as Chanarin-Dorfman syndrome. NLSD is a recessively inherited disorder characterized by the accumulation of cytoplasmic triacylglycerols (TAG) in various cell types, including liver and Schwann cells of myelinated and unmyelinated nerve (63). NLSD patients exhibit an array of clinical symptoms including delayed development, neurologic problems, and skin disorders; these features are reminiscent of the retarded growth, neuropathy, and scruffy coat seen in the *fld/fld* mouse.

The underlying mutation in NLSD has not been identified but, as in *fld/fld* mice, defects in lysosomal acid lipase and increased TAG synthesis have been ruled out; contradictory reports exist concerning impaired fatty acid oxidation in NLSD fibroblasts (64, 65). Several lines of evidence point to impaired hydrolysis of endogenously synthesized TAG, which exist in a metabolic pool distinct from that for exogenously supplied TAG (65, 66). Unlike TAG derived exogenously from lipoproteins, endogenously synthesized TAG normally serves as a source of diacylglycerol for phospholipid biosynthesis. As mentioned earlier, the phospholipid content of peripheral nerve myelin in *fld/fld* mice is reduced (55), an expected consequence of an insufficient supply of diacylglycerol due to reduced TAG hydrolysis. Further biochemical studies, as well as genetic mapping of both NLSD and *fld* genes, will be necessary to clarify the potential relationship between the two mutations.

Toward identification of the fld *gene.* The map location of the *fld* locus has not been reported, but several candidate genes have been ruled out based on their failure to segregate with the mutant phenotype. These include genes for lipoprotein lipase, hepatic lipase, apolipoprotein A-IV, and the *cld* and *Kit* loci (52). Negative linkage has also been demonstrated with regard to other neurological mutants having pathological changes in the peripheral nervous system, including crinkled (*cr*), dystonia musculorum (*dt*), dystrophia muscularis (*dy*), jittery (*ji*), shambling (*shm*), trembler (*Tr*), twitcher (*twi*), and vibrator (*vb*) (55). Although it has been established that the *fld* phenotype results from mutation at a single genetic locus, there is no formal evidence to exclude the possibility that more than one linked gene at that locus might be affected. However, as mutations that involve large chromosomal deletions typically result from induced mutagenesis, this is less likely to be the case for a spontaneous mutation, such as *fld*.

The complexity of the phenotype that makes the *fld* mutation so interesting also complicates efforts to identify the underlying defect. Thus far, characterization of the phenotype at the cellular and molecular level has suggested a number of candidates for the *fld* gene including enzymes involved in fatty acid and triglyceride metabolism, peripheral nerve proteins, and transcription factors that regulate the expression of proteins with altered levels in *fld/fld* tissues. Because of the involvement of several tissues and the detection of numerous proteins and mRNAs with altered expression levels, it is difficult to distinguish the primary defect from secondary responses or compensatory changes. It is possible to test some candidates directly by determining enzyme activity or performing protein function assays. One possible functional assay that we are exploring is complementation of the fatty liver phenotype (i.e., triglyceride accumulation, reduced hepatic lipase activity, elevated apoA-IV expression) by transfection of candidate DNA into cultured hepatocytes from *fld/fld* neonates.

A more general method to screen candidate genes is by testing for genetic linkage with the *fld* locus. Localization of the *fld* locus at high resolution is also required for gene isolation strategies such as positional cloning. Toward this aim, the production of a large intercross is underway between the strain carrying the *fld* mutation, BALB/cByJ-fld, and the strain CAST/Ei, derived from wild mice of the related subspecies *Mus musculus castaneus* (K. Reue, unpublished). Definitive mapping of the *fld* locus will permit the evaluation of candidates that arise from further biochemical studies, and may also reveal new candidates based on map position. It is likely that the best strategy for identification of the *fld* gene will combine genetic techniques to provide linked genetic markers and biochemical/molecular techniques to characterize resulting candidates on a functional level. Identification of the specific mutation underlying the *fld* phenotype is likely to provide new insights and reveal connections between the control of lipid homeostasis in newborn animals and the pathogenesis of peripheral neuropathy associated with dyslipidemia.

Combined lipase deficiency

Combined lipase deficiency is caused by a recessive mutation (*cld*) that virtually abolishes the activity of two key enzymes involved in circulating lipid metabolism, lipoprotein lipase (LPL) and hepatic lipase (HL). Tissues of mice homozygous for the *cld* mutation secrete very little active LPL or HL, and consequently develop a severe hypertriglyceridemia; capillaries in *cld/cld* mice become packed with irregularly shaped and coalesced chylomicrons that eventually leads to cyanosis, ischemia, and death 2–3 days postpartum. In this last section of the review, we will focus on several aspects of combined lipase deficiency, including the resultant hyperlipidemia, the genetics underlying the discovery of the *cld* mutation, and its effect on LPL and HL expression. Some possible candidates underlying the molecular defect in combined lipase deficiency will also be discussed.

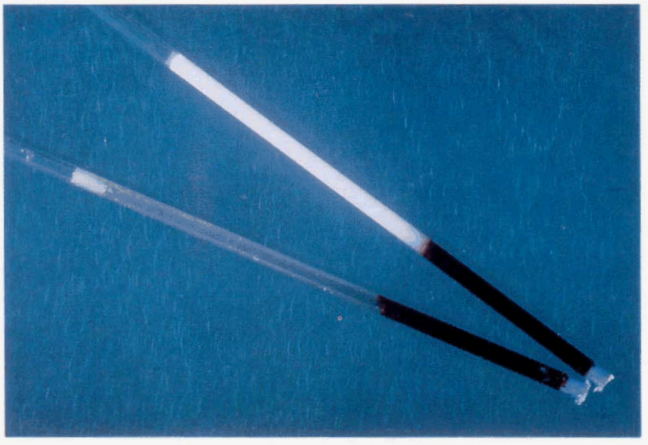

Fig. 4. Hyperchylomicronemia in *cld/cld* neonates 24 h postpartum. Shown are microhematocrit tubes containing blood from *cld/cld* (top) and unaffected (bottom) littermates. The tubes were then centrifuged for 5 min to separate blood cells from plasma; under these conditions, chylomicrons form a white layer above the plasma. The severe hyperchylomicronemia is readily apparent in the sample from the *cld/cld* mouse.

Hyperlipidemia in combined lipase deficiency. The earliest gross characteristic of *cld/cld* mice, besides the tailless condition (see below), is the massive hyperlipidemia evident shortly after birth (**Fig. 4**). This hyperlipidemia is analogous to Type I hyperchylomicronemia in humans, and is due to the severe LPL deficiency manifested in mice carrying two copies of the defective allele. Affected mice show a progressive increase of circulating triglyceride levels, starting at around 4,000 mg/dl, 6–8 h after birth, and often soaring to levels over 20,000 mg/dl at 24–48 h postpartum; cholesterol levels are also increased, starting at approximately 60 mg/dl in utero and increasing 48 h after birth to about 450 mg/dl (51). While the chylomicronemia is the most obvious lipoprotein abnormality present in *cld/cld* mice, the levels of the alpha-lipoproteins (HDL) and pre-beta-lipoproteins (VLDL) were reported to be reduced when compared to unaffected controls (51).

In affected mice, the lumina of capillaries and sinusoids are densely packed with irregularly shaped, nonspherical chylomicrons that contrast sharply with the few spherically shaped chylomicrons present in the capillaries and lacteals of unaffected littermates (67). These abnormally shaped chylomicrons are consistent with an increased surface-to-core ratio, although the reason for this redundant surface is unclear. Perhaps the

small amount of LPL still present in *cld* post-heparin plasma (about 5% of unaffected controls), while inadequate for rates of chylomicron clearance, is sufficient to reduce the surface-to-core ratio of these particles. However, nonspherical chylomicrons are also present in the lacteals of affected mice (67), suggesting that chylomicron assembly in the enterocytes may also be disturbed. Ultrastructural analysis has also shown that chylomicrons extend into extracellular spaces, such as lung alveoli and the space of Disse in liver, while red blood cells are often separated from the surfaces of capillary endothelium due to the dense packing of chylomicrons filling the majority of available space (67). This latter feature, which increases blood viscosity and may disrupt effective gas exchange in alveolar capillaries, might explain the cyanosis evident in *cld/cld* neonates exhibiting severe chylomicronemia.

In contrast to the chylomicronemia, intracellular lipid droplets are rarely seen in tissues of *cld/cld* mice. Even the lipid droplets in brown adipocytes are strikingly reduced in size and number (67), again reflecting the virtual absence of LPL activity in affected animals. Livers of *cld/cld* mice also exhibit a severe reduction in the number of nascent VLDL present in endoplasmic reticulum (ER) and Golgi, and these nascent VLDL are small and irregular in shape (67). Moreover, livers from affected mice begin to show a progressive increase in the numbers of lysosomes as early as 3 h after birth, and many contain lipoprotein particles, lipid spheres, and lamellar structures (67). It remains to be determined whether features such as the apparent reduction of VLDL synthesis and the lysosomal proliferation are primary or secondary affects of the *cld* mutation on liver lipid homeostasis. However, it seems clear that most of these defects occur following ingestion of dietary lipid; tissues of cesarean-derived *cld/cld* mice do not show any of the abnormalities characteristic of the suckling, postnatal animals (67).

While HL activity is also significantly reduced in *cld/cld* mice (51), the overwhelming abnormalities arising from the LPL deficiency mask any contribution of HL deficiency to the overall lipid phenotype. As homozygous disruption of the HL gene in mice causes only mild increases in plasma cholesterol with no change in triglyceride levels (68), HL deficiency undoubtedly contributes little to the overall lipid abnormalities in *cld/cld* mice. In contrast, mice carrying two copies of a disrupted LPL gene suffer a phenotype almost indistinguishable from mice homozygous for the *cld* mutation, including lethality 24–48 h postpartum (69).

Genetics of combined lipase deficiency. Most naturally occurring recessive mutations in mice are detected spontaneously as a consequence of laboratory inbreeding. However, combined lipase deficiency is an example of a highly unusual "parasitic" mutation that was uncovered only after the genetic dissection of a remarkable stretch of DNA called the *t* complex. We will briefly review the salient features of the *t* complex that led to the discovery of the *cld* mutation, as well as the position of markers surrounding *cld*.

Historically, the *t* complex was thought to be a single recessive allele of the *T* (*Brachyury*) locus on chromosome 17 (70). Because *T/t* influenced tail length, these alleles were known as tail interaction factors. In combination with the wild-type allele (+), *T* and *t* produced full, short, and tailless phenotypes (**Fig. 5**). Surprisingly, while *T* turned out to be a mutation within the *Brachyrury* gene that affected mesoderm formation (71), *t* was found not to be a gene at all, but rather a large 15 cM (roughly 35 megabase) region containing a series of four contiguous inversions; indeed, the *t* complex comprises in all about 30% of chromosome 17 (9, 72). An important consequence of these inversions is to exclude the *t* region from normal recombination with noninverted (wild type) DNA during meiosis because of the inability of this region to pair during Prophase I of meiosis (70, 74).

The *t* complex originated some 3 million years ago, and late in its evolution (0.8 million years ago) split into 16 complementing *t* haplotypes (75). During this relatively short time, the various *t* haplotypes have accumulated recessive lethal mutations that have been evolutionarily retained due to the exclusion of the *t* complex from meiotic recombination (75). A consequence of the recessive nature of these lethal mutations is that mice heterozygous for a *t* haplotype and a wild-type chromosome 17 develop and survive normally. Mice can also

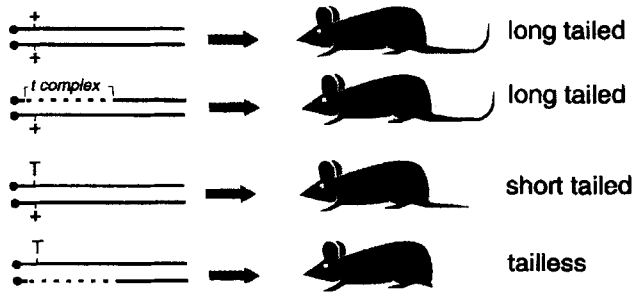

Fig. 5. The *T* gene interacting with the *t* complex influences tail length. Tail length was an important phenotypic marker used in uncovering the *cld* mutation (see text and Fig. 6). The solid and dotted lines represent normal and *t* complex DNA, respectively, on chromosome 17, and the black dot represents the centromeres (which are telomeric in mice). The *t* complex starts about 3 cM from the centromere and ends about 20 cM from the centromere (chromosome 17 is approximately 57 cM in length). The + indicates the position of the wild type *Brachyury* gene, located about 4 cM from the centromere, and *T* represents a mutation within this gene. While *T/T* is an embryonal lethal, *T/+* or *T* in conjunction with the *t* complex affects tail length as shown in this figure.

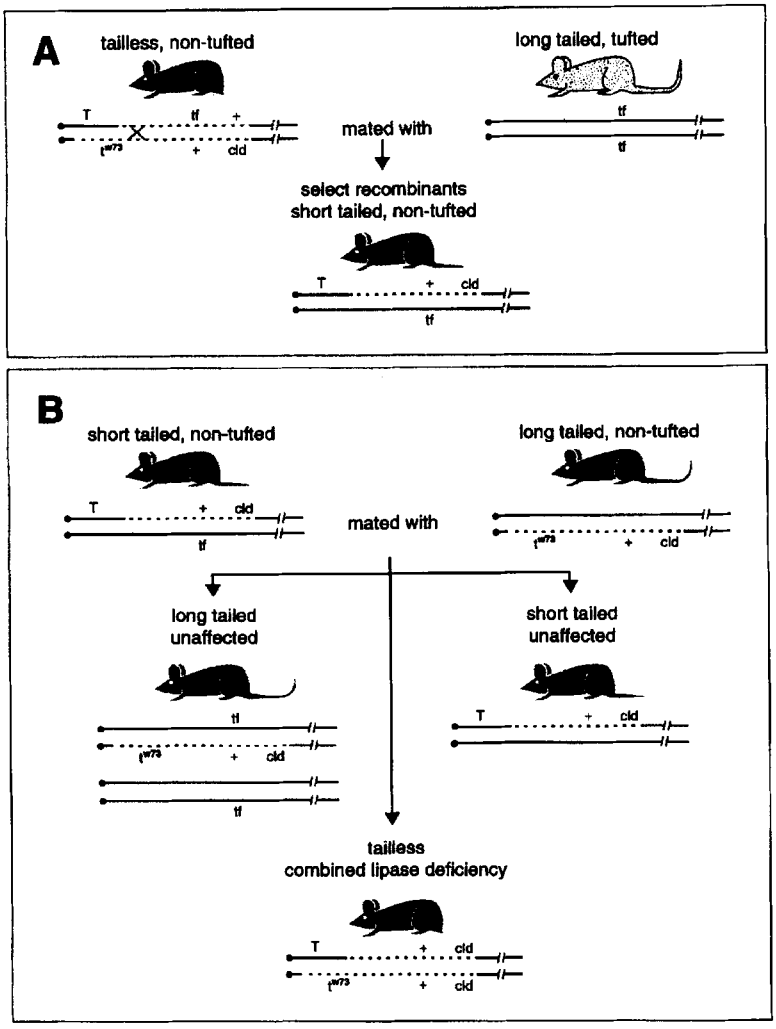

Fig. 6. Uncovering *cld* as a second mutation on the t^{w73} haplotype. (A) The *cld* mutation was uncovered after first removing the embryonic lethal t^{w73} mutation by recombination. Tail length (see Fig. 5) and a second recessive mutation that affects hair pattern, called tufted (*tf*), were used to select appropriate recombinants: animals that no longer contained t^{w73} but still retained *cld* were selected as short-tailed, non-tufted progeny (the "X" in the tailless, non-tufted parent represents the position of the recombination event). (B) Short-tailed, non-tufted recombinants were mated back to mice carrying the original t^{w73} haplotype. Tail length was used to distinguish the three possible genotypes of the resultant progeny (see Fig. 5). Tailless mice that are homozygous for the distal portion of the t^{w73} haplotype died 3 days after birth. This indicated the presence of a second, recessive lethal mutation on the t^{w73} haplotype, later termed *cld*.

survive the inheritance of two distinct *t* haplotypes if each haplotype carries an independent mutation. Moreover, in mice carrying such complementing *t* haplotypes, the regions of inverted DNA can align properly during meiotic prophase and undergo normal crossing over. This ability of complementing *t* haplotypes to recombine permitted genetic mapping of *t* complex mutations; thus far, over 20 lethal or semilethal mutations have been identified (76).

In this manner, combined lipase deficiency was uncovered by Paterniti et al. (51) and Artzt (74) as a second mutation occurring within the t^{w73} haplotype. This haplotype contains the t^{w73} lethal mutation that interrupts normal embryonal development in homozygotes 6 days after fertilization. As illustrated in **Fig. 6A,** the t^{w73} mutation was genetically removed by selecting appropriate recombinants based on tail length and a second phenotypic marker, tufted (*tf*) which affects hair pattern.[1] Artzt (74) found that when these recombinants were mated back to the original t^{w73} haplotype, tailless progeny failed to survive beyond 2 days (Fig. 6B). These results indicated that a second, later acting lethal mutation, *cld,* was present on the original t^{w73} haplotype.

At present, the *cld* mutation has been mapped with respect to tufted (*tf*) as well as two deletions occurring within the *t* haplotypes t^{h20} and t^{w18}. The *cld* mutation was found to be 2.4 cM from *tf* and located within the last inversion of the *t* complex (74). As neither t^{h20} nor t^{w18} were found to remove *cld* (72), these deletions were determined to flank *cld* on either side. Based on these findings, *cld* has been placed 11.5 cM from the cen-

[1]The origin of the tailless, non-tufted parent in Fig. 6A carries two copies of chromosome 17, each with a different (complementing) *t* haplotype: the haplotype containing the *T tf* + alleles was derived by Artzt, McCormick, and Bennet (119) from a *t* complementation group called t^{w12}; the second haplotype called t^{w73} and containing the t^{w73} + *cld* alleles was found in a population of wild mice in Denmark in 1969 (120). The second parent in Fig. 6A (long-tailed, tufted) contains *tf,* a mutation that most likely arose spontaneously in a multiple recessive stock (9). As the *tf* mutation has a high degree of penetrance and does not affect viability, it has been used often to monitor recombinant haplotypes.

tromere on the wild-type (noninverted) chromosome 17 (73) (**Fig. 7**). Unfortunately, finer mapping of the *cld* mutation by classical approaches such as interspecific crosses has not been done because of the difficulty posed by recombination suppression of the *t* complex. Thus, the position of the *cld* mutation at 11.5 cM must be considered tentative, and could vary as much as 1–2 cM on either side. Two mouse homologs of human genes, *Tsc2* and *sazD,* are closely linked to markers within the *cld* region, and suggest that this region may be syntenic to human chromosome 16p13 (77, 78).

LPL and HL expression in combined lipase deficiency. As mentioned previously, LPL and HL activities are significantly reduced in *cld/cld* mice. In the original report on the *cld* mutation by Paterniti et al. (51) LPL and HL activity levels measured in heart, liver and remaining carcass were between 5–20% of the levels in unaffected littermates. The magnitude of this reduction was unchanged in both cesarean-derived and newborn, suckling mice, indicating that the lipase deficiency is present in utero and not affected by the dietary influx of fat or other exogenous factors. Moreover, tissue homogenates from affected mice added back to control samples did not reduce LPL activity, ruling out the possibility of a specific inhibitor in tissues of *cld/cld* mice (51).

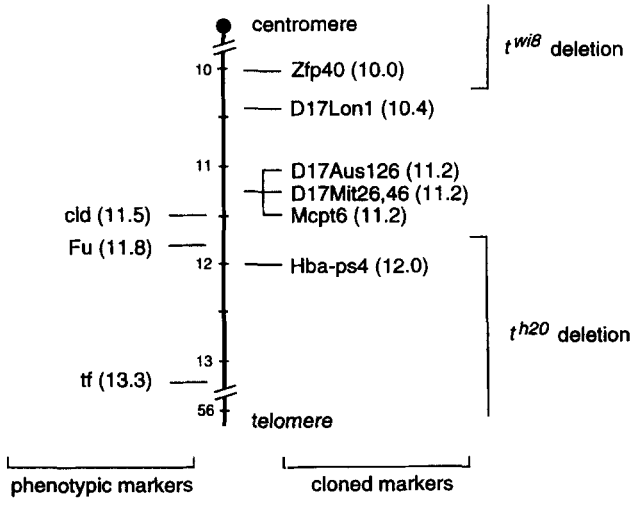

Fig. 7. The region of chromosome 17 carrying the *cld* mutation. Shown is a 4 cM region of chromosome 17 in the vicinity of the *cld* mutation. Cloned DNA markers are shown on the right side of the figure while mutant phenotypes are shown on the left. Numbers in parentheses are the distance of the maker (in cM) from the centromere. The cloned and phenotypic markers are ordered as they would appear on a wild-type (noninverted) chromosome; the markers would be inverted on the *t* complex. The identity of the cloned markers are as follows: *Zfp40,* a zinc finger protein; *D17Lon1,* a YAC end fragment; *D17Aus126, D17Mit26,* and *D17Mit46,* simple sequence length polymorphisms; *Mcpt6,* a mast cell protease; and *Hba-ps4,* a pseudogene of hemoglobin A. The phenotypic markers are: *cld,* combined lipase deficiency; *Fu,* a dominant mutation that affects skeletal development; and *tf,* a recessive mutation affecting hair pattern. The t^{w18} deletion removes *Zfp40* but not *D17Lon1* or *cld;* the t^{h20} deletion removes *Fu, Hba-ps4,* and *tf* but not *cld.*

Later reports by Olivecrona, Scow and their colleagues confirmed that LPL and HL activity levels are reduced in a number of tissues from affected mice, including diaphragm muscle, heart, brown adipose tissue, and liver as well as postheparin plasma (67, 79–81). Using specific antibodies, they found that the small amount of lipolytic activity in *cld* tissues was attributable to LPL and HL (14, 80), and also found a surprisingly high amount of LPL activity in affected liver (40% of unaffected controls) (80). Importantly, Blanchette-Mackie et al. (67) showed that the addition of bovine LPL to chylomicrons isolated from *cld/cld* mice resulted in the release of free fatty acids at rates comparable to unaffected controls; moreover, the addition of a source of apolipoprotein C-II (heat-inactivated rat serum) to these chylomicrons did not increase the rate of triglyceride hydrolysis. Thus, the hyperchylomicronemia present in *cld/cld* mice is not due to either substrate or cofactor insufficiencies, but must result exclusively from diminished LPL activity.

Unlike the reduction in enzyme activity, LPL protein was reported to be expressed at normal to supranormal levels in the tissues of affected mice (79, 81, 82). Using a crude immunoassay, Olivecrona et al. (79) detected levels of LPL protein that were 4- to 8-fold higher in tissues from affected mice when compared to unaffected controls. While these authors did not report values of enzyme specific activity, their measurement of LPL activity in heart (2.5% of unaffected controls) when compared to their measurement of LPL protein (680% of unaffected controls) clearly indicates the presence of significant amounts of inactive enzyme mass. Davis et al. (82) directly measured LPL specific activity in heart, kidney, and brain and found it to be 3–15% of unaffected controls, confirming the presence of inactive LPL mass in the tissues of *cld* mice. However, these authors also found that the small amount of lipase activity in *cld* postheparin plasma was balanced by an equally small amount of detectable mass, suggesting that secreted LPL retains a normal specific activity (82).

LPL and HL mRNA levels and rates of synthesis were also found to be normal to high in tissues of *cld/cld* mice. Although not quantitated, Northern blots reported by Oka et al. (83, 84) indicated that levels of LPL and HL mRNA were significantly elevated in tissues of affected mice when compared to unaffected controls. In contrast, Davis et al. (82) also using Northern blot analysis, showed that LPL and HL mRNA levels were essentially unchanged. Like mRNA levels, the measurement of LPL and HL synthetic rates by the incorporation of [^{35}S]methionine showed that lipase production was unchanged to elevated in tissues of *cld/cld* mice (79, 82).

Taken together, these results indicated that combined lipase deficiency did not result from impaired lipase production rates but rather from the production of enzymatically inactive protein. As dysfunctional proteins often result from mutations affecting coding sequence, it was proposed early on that the *cld* mutation may directly disrupt the lipase structural genes (51, 79). This possibility has now been unequivocally ruled out by various lines of evidence. First, the mapping of the LPL and HL structural genes to mouse chromosomes 8 and 9, respectively (85, 86), has shown that the *cld* mutation on chromosome 17 must be acting in trans to affect lipase activity. Second, no insertions or deletions in the LPL gene were detected when Southern blots of *cld/cld* and unaffected DNA were digested with 16 different endonucleases (83). Third, a ribonuclease A protection assay, carried out with HL mRNA from *cld* liver hybridized to a normal mouse HL cDNA clone, did not uncover any point mutations, indicating that the HL gene and resultant mRNA were not affected by the *cld* mutation (84). Thus, alterations of lipase primary amino acid sequence can be eliminated as the cause of LPL and HL dysfunction in combined lipase deficiency.

A second possibility put forth by several investigators was that the *cld* mutation might disrupt a co- or post-translational step essential for the maturation of nascent LPL and HL polypeptides to catalytically active molecules. The step proposed to be defective was asparagine-linked glycosylation (51, 79, 81, 82, 87). This hypothesis was attractive as there was emerging evidence that the addition of *N*-linked oligosaccaharides was an important step for the expression of lipase activity (88–93). Site-directed mutagenesis later confirmed that glycosylation of the *N*-terminal domains of both LPL and HL was essential for their activity (94–96). Moreover, it was found that inhibition of the first step in glycan processing reduced LPL and HL specific activities substantially (97–99). Finally, early studies examining antigens associated with various *t* haplotypes indicated that they differed with respect to their content of terminal carbohydrates (100), hinting that mutations within this region may affect glycosylation and therefore reduce lipase specific activity.

Asparagine-linked glycosylation begins in the ER with the co-translational transfer of a core glycan unit comprised of 2 N-acetylglucosamine (GlcNAc) residues, 9 mannose (Man) residues, and 3 glucose (Glu) residues ($Glc_3Man_9GlcNAc_2$) to the appropriate asparagine residues of a growing polypeptide chain. Processing of this "core high mannose" group also begins in the ER by the sequential removal of the terminal glucose residues followed by initial mannose cleavage; cleavage of the final mannose residues is accomplished in the *cis*-Golgi to yield $Man_5GlcNAc_2$. Addition of outer carbohydrate residues, including galactose and sialic acid, occurs in the *medial/trans*-Golgi. The glycan structures $Glc_3Man_9GlcNAc_2$ through $Man_5GlcNAc_2$ are called "high mannose" structures that are processed to "complex" structures by the addition of the outer carbohydrate residues in Golgi.

Studies by Masuno et al. (81) and Davis et al. (82) clearly showed that core high mannose groups were added to newly synthesized LPL and HL in tissues of *cld/cld* mice. What they found, however, was that the LPL and HL oligosaccharides were never processed past the high mannose stage. This phenotype was also seen when a *cld/cld* cell line developed in our laboratory was transfected with human LPL cDNA (**Fig. 8**). These data suggested two alternative explanations: *a) cld/cld* cells were unable to convert high mannose forms to complex structures; or *b)* that LPL and HL were retained within the ER and never reached *medial/trans*-Golgi to become processed to complex forms. Davis et al. (82) showed that adipsin, a secreted *N*-linked glycoprotein synthesized by adipose tissue and sciatic nerve, possessed fully processed complex glycan structures in *cld* plasma. While this result cannot unequivocally rule out a defect in the ability to process high mannose chains to complex forms in the tissues specifically expressing LPL and HL, it suggests that the *cld* mutation does not globally affect the processing of all glycoproteins.

Importantly, the inability to convert high mannose forms to complex structures could only explain combined lipase deficiency if this failure affected the maturation of LPL and HL to active, secreted enzymes.

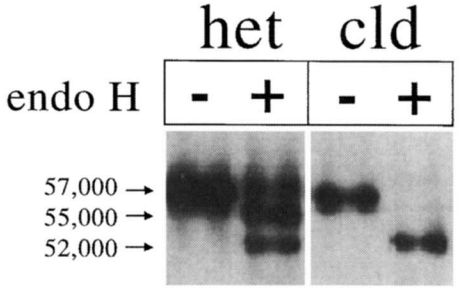

Fig. 8. LPL posttranslational processing in unaffected and *cld/cld* cells. Fibroblast cell lines were developed from *cld/cld* and unaffected littermates from skin. Unaffected cells are heterozygous for the *cld* mutation and are labeled as het. Het and cld cell lines, transfected with a human LPL cDNA clone, were homogenized in the presence of detergents and immunoprecipitated with antibodies specific for LPL. Immunoprecipitates were then subjected to digestion with the glycosidase endoglycosidase H; complex glycan chains are resistant to endo H cleavage whereas high mannose chains are readily removed. The samples were finally separated on SDS polyacrylamide gels and subjected to Western blot analysis using LPL specific antibodies. In the endo H + lanes, the 57,000 and 55,000 dalton bands represent LPL containing complex oligosaccharides; the 52,000 dalton band represents LPL with high mannose residues. See text for additional details.

However, Ben-Zeev et al. (97) showed that maturation of LPL occurs within the ER, and that conversion to the complex form is not required. Only the initial processing step in ER has been shown to be important: the removal of the terminal glucose residues of LPL high mannose forms by the ER glucosidases I and II are necessary for their full maturation to catalytically active molecules (97–99). The necessity for the removal of these terminal glucose residues may reflect the requirement of LPL and HL to interact with the ER chaperone, calnexin; interaction of nascent glycoproteins with calnexin has been shown to be dependent on the removal of the outer two glucose residues (101, 102).

While it remains a formal possibility that combined lipase deficiency results from defective glucose trimming, several observations make it unlikely. First, inhibition of the glucose trimming does not only affect LPL and HL, but many *N*-linked glycoproteins (101, 102). As yet, no other proteins besides LPL and HL have been shown to be affected by the *cld* mutation. Second, because of the requirement of this step for the interaction of many nascent glycoproteins with calnexin, it is very likely that failure of terminal glucose cleavage would be catastrophic for normal fetal development; indeed, disruption of calnexin is lethal in the yeast *Schizosaccharomyces pombe* (103). Although combined lipase deficiency is lethal, death occurs postnatally and is almost certainly due to the LPL deficiency acting alone (69). Average litter size from heterozygous matings (+/*cld* × +/*cld*) are as large as litters from matings that cannot give rise to *cld/cld* pups (+/*cld* × +/+), indicating that the *cld* mutation does not adversely affect fetal development (51).

The observed failure of LPL and HL high mannose forms to be further processed could result from the retention of these lipases within the ER of *cld/cld* cells. Indeed, Masuno et al. (81) showed that the distribution of LPL within *cld/cld* brown adipocytes is reticular in appearance, consistent with its presence in ER. Retention of proteins often results from quality control mechanisms operating within the ER that prevent the entry of misfolded proteins to Golgi (104–106). Consequently, we hypothesize that the *cld* mutation causes the disruption of a step that is critical for the attainment of a proper tertiary or quaternary lipase structure, resulting in its retention in the ER. Consistent with this hypothesis is the observation that LPL from *cld/cld* brown adipocytes appears to elute from heparin-Sepharose at a reduced ionic strength (81). This could mean that either LPL has failed to dimerize (107), or that regions within LPL critical for heparin binding are misfolded and thus bind heparin with reduced affinity. Further investigation will be required to determine unequivocally whether LPL and HL in *cld/cld* cells are present as misfolded proteins.

Molecular defect in combined lipase deficiency. Although the gene affected by the *cld* mutation awaits identification, possible candidates include chaperones or other ER proteins involved in the folding of nascent polypeptides to fully functional enzymes. Among the chaperones and heat shock proteins that have been mapped in the mouse, some are located to chromosome 17. For example, the genes for three heat shock proteins (Hsp70-1, Hsp70t, and Hsp70-3) are located on chromosome 17 in a linkage group 18–20 cM from the centromere (73, 108). The *Tcp1* gene, a cytoplasmic chaperone, is also present on chromosome 17 about 7.5 cM from the centromere (73, 109). As *cld* has been mapped to a region 11.5 cM from the centromere (Fig. 7), these genes are not strong candidates. Nevertheless, other chaperones and protein folding enzymes have not yet been mapped in the mouse. These include ERp59, also called protein disulfide isomerase (PDI), which is involved in folding of a variety of proteins by catalyzing the isomerization of intramolecular disulfide bridges (110). ERp72 and ERp61 are characterized by the presence of conserved sequences corresponding to the active sites of PDI (111, 112). ERp99, also called Grp94, belongs to the heat shock protein 90 family of stress proteins (113). As mentioned earlier, calnexin is an ER chaperone that interacts with *N*-linked glycoproteins (102). Finally, genes encoding proteins involved in protein trafficking may also be candidates. For example, ERGIC-53 is a lectin-like protein, located within the intermediate (ER-to-Golgi) compartment, that has been proposed to be involved in the translocation of *N*-linked glycoproteins to Golgi after their interaction with calnexin (114). Before any of these genes can be considered as viable candidates for the *cld* gene, they must be able to explain the apparent specificity of the mutation for the two lipases. Perhaps the *cld* gene product will turn out to be analogous to the receptor-associated protein (RAP) which has been suggested to be a specific chaperone for the low density lipoprotein receptor-related protein (115, 116).

Future directions. The ultimate challenge in understanding the etiology of combined lipase deficiency will be determining the gene affected by the *cld* mutation. Pure genetic approaches such as positional cloning require the identification of DNA markers, closely linked to the mutation, that provide a practical molecular approach towards the affected gene. This is accomplished by mapping DNA markers with respect to the mutation of interest in a large genetic cross. Obviously, DNA markers can be followed in a cross only if the parental alleles of that marker are distinguishable as DNA fragments varying in size (i.e., simple sequence length polymorphisms). For this reason, interspecific crosses with *Mus spretus* or *Mus castaneus* are generally

utilized to maximize the number of informative polymorphic markers. Unfortunately, an interspecific cross with *cld* mice would not yield recombinants in the region of the *cld* mutation, as the inversions within the *t* complex prohibits crossing over with the wild-type chromosome 17 present in *M. spretus* and *M. castaneus*. While mapping can be accomplished by producing crosses in strains containing complementing *t* haplotypes, the recent evolutionary divergence of the various haplotypes greatly reduce the chance that markers within the *t* complex region will be polymorphic.

Because of these difficulties, we have planned to identify the *cld* gene by combining a positional cloning approach with genetic complementation. Using yeast artifical chromosome (YAC) clones, we are constructing a series of overlapping YAC clones (called a YAC contig) that cover the region between the two deletions t^{w18} and t^{h20}. This will assure that the YAC contig contains the *cld* gene (Fig. 7). To identify which individual YAC clone from this contig carries the *cld* wene, we are taking advantage of our fibroblast cell line that expresses the mutation (Fig. 8). YAC clones retrofitted with a mammalian selectable marker (neomycin resistance) will be expressed in the *cld/cld* cell line; YAC clones containing a functional copy of the *cld* gene will be identified by their ability to complement the recessive phenotype, thus permitting the secretion of catalytically active LPL from *cld/cld* cells. Once a complementing YAC clone is identified, the YAC can be used to select for cDNA clones corresponding to genes contained within that YAC. Expression of these candidate cDNA clones in *cld/cld* cells can be used to finally identify a complementing cDNA clone representing the *cld* gene product.

Concluding remarks

We have reviewed the naturally occurring mutations in mice that affect lipid transport and metabolism because they provide a means of identifying novel genes and processes. By their very nature, spontaneously arising mutations are identified only when they disrupt genes necessary in the maintenance of some aspect of lipid homeostasis. Together with induced mutations and transgenic models, naturally occurring mutations furnish complementary approaches for determining function. The ease of linkage mapping in mice and the constantly increasing coverage of the mouse genome by YAC contigs are making the identification of novel genes by positional cloning a reasonable goal. Moreover, new techniques are continually being developed that will also steadily increase the likelihood of success, such as genetically directed representational difference analysis (117). As lipid metabolism is characterized by complex interacting pathways that are regulated at many points, naturally occurring mutations provide a powerful means of identifying some of the key genes controlling these pathways.

This work was supported by National Institutes of Health Grant HL28482. K. R. and M. H. D. are Established Investigators of the American Heart Association.

Manuscript received 8 February 1996 and in revised form 22 April 1996.

REFERENCES

1. Zannis, V. I., and J. L. Breslow. 1985. Genetic mutations affecting human lipoprotein metabolism. *In* Advances in Human Genetics. H. Harris and K. Hirschhorn, editors. Plenum Publishing Corporation, New York. 125–215.
2. Ishida, B., and B. Paigen. 1981. Atherosclerosis in the mouse. *In* Genetic Factors in Atherosclerosis: Approaches and Model Systems. A. J. Lusis and R. S. Sparkes, editors. Kargel, AG, Basel. 189–222.
3. Reue, K., C. H. Warden, and A. J. Lusis. 1990. Animal models for genetic lipoprotein defects. *Curr. Opin. Lipidol.* **1:** 143–150.
4. Van Lenten, B. J. 1989. Animal models: the Watanabe heritable hyperlipidemic rabbit. *In* Genetic Factors in Atherosclerosis: Approaches and Model Systems. A. J. Lusis and R. S. Sparkes, editors. Kargel, AG, Basel. 125–138.
5. Laber-Laird, K., and L. L. Rudel. 1989. Genetic aspects of plasma lipoprotein and cholesterol metabolism in nonhuman primate models of atherosclerosis. *In* Genetic Factors in Atherosclerosis: Approaches and Model Systems. A. J. Lusis and R. S. Sparkes, editors. Kargel, AG, Basel. 170–188.
6. Racpacz, J., and J. Hasler-Rapacz. 1989. Animal models: the pig. *In* Genetic Factors in Atherosclerosis: Approaches and Model Systems. A. J. Lusis and R. S. Sparkes, editors. Kargel, AG, Basel. 139–169.
7. Silver, L. M. 1995. Mouse Genetics. Concepts and Applications. Oxford University Press, New York.
8. Festing, M. F. W. 1989. Inbred strains of mice. *In* Genetic Variants and Strains of the Laboratory Mouse. 2nd edition. M. F. Lyon and A. G. Searle, editors. Oxford University Press, New York. 636–648.
9. Green, M. C. 1989. Catalog of mutant genes and polymorphic loci. *In* Genetic Variants and Strains of the Laboratory Mouse. 2nd edition. M. F. Lyon and A. G. Searle, editors. Oxford University Press, New York. 12–403.
10. Avner, P., L. Amar, L. Dandolo, and J. L. Guénet. 1988. Genetic analysis of the mouse using interspecific crosses. *Trends Genet.* **4:** 18–23.
11. Dietrich, W. F., N. G. Copeland, D. J. Gilber, J. C. Miller, N. A. Jenkins, and E. S. Lander. 1995. Mapping the mouse genome: current status and future prospects. *Proc. Natl. Acad. Sci. USA.* **92:** 10849–10853.
12. Lander, E. S., and N. J. Schork. 1994. Genetic dissection of complex traits. *Science.* **265:** 2037–2048.
13. Breslow, J. L. 1994. Insights into lipoprotein metabolism from studies in transgenic mice. *Annu. Rev. Physiol.* **56:** 797–810.
14. Smithies, O., and N. Maeda. 1995. Gene targeting approaches to complex genetic diseases: atherosclerosis and

essential hypertension. *Proc. Natl. Acad. Sci. USA.* **92:** 5266–5272.
15. Paigen, B., A. S. Plump, and E. M. Rubin. 1994. The mouse as a model for human cardiovascular disease and hyperlipidemia. *Curr. Opin. Lipidol.* **5:** 258–264.
16. Paigen, B. 1995. Genetics of responsiveness to high-fat and high-cholesterol diets in the mouse. *Am. J. Clin. Nutr.* **62:** 458S–462S.
17. Shih, D. M., C. Welch, and A. J. Lusis. 1995. New insights into atherosclerosis from studies with mouse models. *Mol. Med. Today.* **1:** 364–372.
18. Friedman, J. M., and R. L. Leibel. 1992. Tackling a weighty problem. *Cell.* **69:** 217–220.
19. Leiter, E. H. 1993. Obesity genes and diabetes induction in the mouse. *Crit. Rev. Food Sci. Nutr.* **33:** 333–338.
20. Keightly, P. D. 1995. Chewing the fat. *Nat. Genet.* **10:** 125–126.
21. Geissler, E. N., M. A. Ryan, and D. E. Housman. 1988. The dominant-white spotting locus of the mouse encodes the c-Kit proto-oncogene. *Cell.* **55:** 185–192.
22. Hinsdale, M. E., C. L. Kelly, and P. A. Wood. 1993. Null allele at *Bcd-1* locus in BALB/cByJ mice is due to a deletion in the short-chain acyl-CoA dehydrogenase gene and results in missplicing of mRNA. *Genomics.* **16:** 605–611.
23. Pentchev, P. G., M. T. Vanier, K. Suzuki, and M. C. Patterson. 1995. Niemann-Pick Disease Type C: a cellular cholesterol lipidosis. *In* Metabolic Basis of Inherited Disease. 7th edition, C. R. Scrivner, A. L. Beaudet, W. S. Sly, and D. Valle, editors. McGraw-Hill, New York. 2625–2639.
24. Miyawaki, S., S. Matsuoka, T. Sakiyama, and T. Kitagawa. 1982. Sphingomyelinosis, a new mutation in the mouse. A model of Niemann-Pick disease in humans. *J. Hered.* **73:** 257–263.
25. Morris, M. D., C. Bhuvaneswaran, H. Shio, and S. Fowler. 1982. Lysosome lipid storage disorder in NCTR-BALB/c mice. I. Description of the disease and genetics. *Am. J. Pathol.* **108:** 140–149.
26. Adachi, M., B. W. Volk, and L. Schneck. 1976. Niemann-Pick disease type C. Animal model: mouse Niemann-Pick disease. *Am. J. Pathol.* **85:** 229–231.
27. Shio, H., S. Fowler, C. Bhuvaneswaran, and M. D. Morris. 1982. Lysosome lipid storage disorder in NCTR-BALB/c mice. II. Morphological and cytochemical studies. *Am. J. Pathol.* **108:** 150–159.
28. Miyawaki, S., H. Yoshida, and S. Mitsuoka. 1986. A model for Niemann-Pick disease. Influence of genetic background on disease expression in *spm/spm* mice. *J. Hered.* **77:** 379–384.
29. Pentchev, P. G., M. C. Comly, H. S. Kruth, S. Patel, M. Proestel, and H. Weintroub. 1986. The cholesterol storage disorder of the mutant BALB/c mouse. A primary genetic lesion closely linked to defective esterification of exogenously derived cholesterol and its relationship to human type C Niemann-Pick disease. *J. Biol. Chem.* **261:** 2772–2777.
30. Ohno, K., E. Nanba, S. Miyawaki, T. Sakiyama, T. Kitagawa, and K. Takeshita. 1992. A cell line from sphingomyelinosis mouse shows alterations in intracellular cholesterol metabolism similar to those in type C Niemann-Pick disease. *Cell Struct. Funct.* **17:** 229–235.
31. Horinuchi, K., T. Sakiyama, L. Pereira, P. A. Lally, and E. H. Schuchman. 1993. Mouse models of Niemann-Pick disease: mutation analysis and chromosomal mapping rule out the type A and B forms. *Genomics.* **18:** 450–451.
32. Otterbach, B., and W. Stoffel. 1995. Acid sphingomyelinase-deficient mice mimic the neurovisceral form of human lysosomal storage disease (Niemann-Pick disease). *Cell.* **81:** 1053–1061.
33. Kurimasa, A., K. Ohno, and M. Oshimura. 1993. Restoration of the cholesterol metabolism in 3T3 cell lines derived from the sphingomyelinosis mouse (*spm/spm*) by transfer of a human chromosome 18. *Hum. Genet.* **92:** 157–162.
34. Wood, P. A., B. A. Amendt, W. J. Rhead, D. S. Millington, F. Inoue, and D. Armstrong. 1989. Short-chain acyl-coenzyme A dehydrogenase deficiency in mice. *Pediatr. Res.* **25:** 38–43.
35. Schiffer, S. P., M. Prochazka, P. F. Jezyk, T. H. Roderick, M. Yudkoff, and D. F. Patterson. 1989. Organic aciduria and butyryl CoA dehydrogenase deficiency in BALB/cByJ mice. *Biochem. Genet.* **27:** 47–58.
36. Kuwajima, M., N. Kono, M. Horiuchi, Y. Imamura, A. Ono, Y. Inui, S. Kawata, T. Koizumi, J-I. Hayakawa, T. Saheki, and S. Tarui. 1991. Animal model of systemic carnitine deficiency: analysis in C3H-H-2° strain of mouse associated with juvenile visceral steatosis. *Biochem. Biophys. Res. Commun.* **174:** 1090–1094.
37. Tomomura, M., Y. Imamura, M. Horiuchi, T. Koizumi, H. Nikaido, J-I. Hayakawa, and T. Saheki. 1992. Abnormal expression of urea cycle enzyme genes in juvenile visceral steatosis (*jvs*) mice. *Biochim. Biophys. Acta.* **1138:** 167–171.
38. Horiuchi, M., K. Kobayashi, M. Tomomura, M. Kuwajima, Y. Imamura, T. Koizumi, H. Nikaido, J-I. Hayakawa, and T. Saheki. 1992. Carnitine administration to juvenile visceral steatosis mice corrects the suppressed expression of urea cycle enzymes by normalizing their transcription. *J. Biol. Chem.* **267:** 5032–5035.
39. Horiuchi, M., K. Kobayashi, S. Yamaguchi, N. Shimizu, T. Koizumi, H. Nikaido, J. Hayakawa, M. Kuwajima, and T. Saheki. 1994. Primary defect of juvenile visceral steatosis (*jvs*) mouse with systemic carnitine deficiency is probably in renal carnitine transport system. *Biochim. Biophys. Acta.* **1226:** 25–30.
40. Schiffman, M. B., M. L. Santorineou, S. E. Lewis, H. A. Turchin, and S. Gluecksohn-Waelsch. 1975. Lipid deficiencies, leukocytosis, brittle skin—a lethal syndrome caused by a recessive mutation, edematous (*oed*), in the mouse. *Genetics.* **81:** 525–536.
41. Gluecksohn-Waelsch, S., D. Hagedorn, and B. F. Sisken. 1956. Genetics and morphology of a recessive mutation in the house mouse, affecting head and limb skeleton. *J. Morphol.* **99:** 465–479.
42. Doering, C. H., J. G. M. Shire, S. Kessler, and R. B. Clayton. 1973. Genetic and biochemical studies of the adrenal lipid depletion phenotype in mice. *Biochem. Genet.* **8:** 101–111.
43. Taylor, B. A., H. Meier, and W. K. Whitten. 1974. Chromosomal location and site of action of the adrenal lipid depletion gene of the mouse. *Genetics.* **77:** s65.
44. Welch, C. L., Y-R. Xia, I. Shechter, R. Farese, M. Mehrabian, S. Mehdizadeh, C. H. Warden, and A. J. Lusis. 1996. Genetic regulation of cholesterol homeostasis: chromosomal organization of candidate genes. *J. Lipid Res.* **37:** 1406–1421.
45. Aukema, H. M., T. Yamaguchi, H. Takahashi, B. Celi, and B. J. Holub. 1992. Abnormal lipid and fatty acid compo-

sitions of kidneys from mice with polycystic kidney disease. *Lipids.* **27:** 429–435.

46. Deshmukh, G. D., N. S. Radin, V. H. Gattone, and J. A. Shayman. 1994. Abnormalities of glycosphingolipid, sulfatide, and ceramide in the polycystic (*cpk/cpk*) mouse. *J. Lipid Res.* **35:** 1611–1618.
47. Takahashi, H., J. P. Calvet, D. Dittemore-Hoover, K. Yoshida, J. J. Grantham, and V. H. Gattone II. 1991. A hereditary model of slowly progressive polycystic kidney disease in the mouse. *J. Am. Soc. Nephrol.* **1:** 980–989.
48. Mandell, J., W. K. Koch, R. Nideas, G. M. Preminger, and E. McFarland. 1983. Congenital polycystic kidney disease: genetically transmitted infantile polycystic kidney disease in C57BL/6J mice. *Am. J. Pathol.* **113:** 112–114.
49. Davisson, M. T., L. M. Buay-Woodford, H. W. Harris, and P. D'Eustachio. 1991. The mouse polycystic kidney disease mutation (*cpk*) is located on proximal chromosome 12. *Genomics.* **9:** 778–781.
50. Wallace, M. E., and B. M. Herbertson. 1969. Neonatal intestinal lipidosis in mice. An inherited disorder of the intestinal lymphatic vessels. *J. Med. Genet.* **6:** 361–375.
51. Paterniti, J. R., Jr., W. V. Brown, H. N. Ginsberg, and K. Artzt. 1983. Combined lipase deficiency (*cld*): a lethal mutation on chromosome 17 of the mouse. *Science.* **221:** 167–169.
52. Langner, C. A., E. H. Birkenmeier, O. Ben-Zeev, M. C. Schotz, H. O. Sweet, M. T. Davisson, and J. I. Gordon. 1989. The fatty liver dystrophy (*fld*) mutation. A new mutant mouse with a developmental abnormality in triglyceride metabolism and associated tissue-specific defects in lipoprotein lipase and hepatic lipase activities. *J. Biol. Chem.* **264:** 7994–8003.
53. Hatanaka, K., H. Tanishita, H. Ishibashi-Ueda, and A. Yamamoto. 1986. Hyperlipidemia in mast cell-deficient *W/W*^{v} mice. *Biochim. Biophys. Acta.* **878:** 440–445.
54. Sweet, H. O., E. H. Birkenmeier, and M. T. Davisson. 1988. Fatty liver dystrophy (*fld*). *Mouse News Lett.* **81:** 69.
55. Langner, C. A., E. H. Birkenmeier, K. A. Roth, R. T. Bronson, and J. I. Gordon. 1991. Characterization of the peripheral neuropathy in neonatal and adult mice that are homozygous for the fatty liver dystrophy (*fld*) mutation. *J. Biol. Chem.* **266:** 11955–11964.
56. Reue, K., S. Rehnmark, C. S. Giometti, and M. Doolittle. 1994. The fatty liver dystrophy (*fld*) mutation: a developmental abnormality in fatty acid oxidation. *Circulation.* **90:** I–80.
57. Frost, S. C., W. A. Clark, and M. A. Wells. 1983. Studies on fat digestion, absorption, and transport in the suckling rat. IV. In vivo rates of triacylglycerol secretion by intestine and liver. *J. Lipid Res.* **24:** 899–903.
58. Giese, K. P., R. Martini, G. Lemke, P. Soriano, and M. Schachner. 1992. Mouse P_0 gene disruption leads to hypomyelination, abnormal expression of recognition molecules, and degeneration of myelin and axons. *Cell.* **71:** 565–576.
59. Narayanan, V., K. H. Kaestner, and G. I. Tennekoon. 1991. Structure of the mouse myelin P2 protein gene. *J. Neurochem.* **57:** 75–80.
60. Suter, U., A. A. Welcher, T. Ozcelik, G. J. Snipes, B. Kosaras, U. Franke, S. Billings-Gagliardi, R. K. Sidman, and E. M. Shooter. 1992. Trembler mouse carries a point mutation in a myelin gene. *Nature.* **356:** 241–244.
61. Brown, F. R., R. Voight, A. K. Singh, and I. Singh. 1993. Peroxisomal disorders. Neurodevelopmental and biochemical aspects. *Am. J. Dis. Child.* **147:** 617–626.
62. Hale, D. E., and M. J. Bennett. 1992. Fatty acid oxidation disorders: a new class of metabolic diseases. *J. Pediatr.* **121:** 1–11.
63. Chanarin, I., A. Patel, G. Slavin, E. G. Wills, T. M. Andrews, and G. Steward. 1975. Neutral lipid storage disease: a new disorder of lipid metabolism. *Br. J. Med.* **1:** 553–555.
64. Williams, M. L., D. J. Monger, S. L. Rutherford, M. Hincenbergs, S. J. Rehfeld, and C. Grunfeld. 1988. Neutral lipid storage disease with ichthyosis: lipid content and metabolism of fibroblasts. *J. Inherited Metab. Dis.* **11:** 131–143.
65. Di Donato, S., B. Garavaglia, P. Strisciuglio, C. Borrone, and G. Andria. 1988. Multisystem triglyceride storage disease is due to a specific defect in the degradation of endocellularly synthesized triglycerides. *Neurology.* **38:** 1107–1110.
66. Williams, M. L., R. A. Coleman, D. Placezk, and C. Grunfeld. 1991. Neutral lipid storage disease: a possible functional defect in phospholipid-linked triacylglycerol metabolism. *Biochim. Biophys. Acta.* **1096:** 162–169.
67. Blanchette-Mackie, E. J., M. G. Wetzel, S. S. Chernick, J. R. Paterniti, Jr., W. V. Brown, and R. O. Scow. 1986. Effect of the combined lipase deficiency mutation (*cld/cld*) on ultrastructure of tissues in mice. *Lab. Invest.* **55:** 347–362.
68. Homanics, G. E., H. V. de Silva, J. Osada, S. H. Zhang, H. Wong, and N. Maeda. 1995. Mild dyslipidemia in mice following targeted inactivation of the hepatic lipase gene. *J. Biol. Chem.* **270:** 2974–2980.
69. Coleman, T., R. L. Seip, J. M. Gimble, D. Lee, N. Maeda, and C. F. Semenkovich. 1995. COOH-terminal disruption of lipoprotein lipase in mice is lethal in homozygotes, but heterozygotes have elevated triglycerides and impaired enzyme activity. *J. Biol. Chem.* **270:** 12518–12525.
70. Silver, L. M. 1990. At the crossroads of developmental genetics: the cloning of the classical mouse T locus. *BioEssays.* **8:** 377–380.
71. Herrmann, B. G., S. Labeit, A. Poustka, T. R. King, and H. Lehrach. 1990. Cloning of the T gene required in mesoderm formation in the mouse. *Nature.* **343:** 617–622.
72. Artzt, K., D. Barlow, W. F. Dove, K. F. Lindahl, J. Klein, M. F. Lyon, and L. M. Silver. 1991. Maps of mouse chromosome 17: first report. *Mamm. Genome.* **1:** 5–29.
73. Forejt, J., K. Artzt, D. P. Barlow, R. M. Hamvas, K. F. Lindahl, M. F. Lyon, J. Klein, and L. M. Silver. 1994. Mouse chromosome 17. *Mamm. Genome.* **5:** S238–S258.
74. Artzt, K. 1984. Gene mapping within the T/t complex of the mouse. III: t-Lethal genes are arranged in three clusters on chromosome 17. *Cell.* **39:** 565–572.
75. Morita, T., H. Kubota, K. Murata, M. Nozaki, C. Delarbre, K. Willison, Y. Satta, M. Sakaizumi, N. Takahata, G. Gachelin, and A. Matsushiro. 1992. Evolution of the mouse *t* haplotype: recent and worldwide introgression to *Mus musculus*. *Proc. Natl. Acad. Sci. USA.* **89:** 6851–6855.
76. Vernet, C., and K. Artzt. 1995. Mapping of 12 markers in the proximal region of mouse chromosome 17 using recombinant *t* haplotypes. *Mamm. Genome.* **6:** 219–221.
77. Himmelbauer, H., M. Pohlschmidt, A. Snarey, G. G. Germino, D. Weinstat-Saslow, S. Somlo, S. T. Reeders, and A-M. Frischauf. 1992. Human–mouse homologies in

the region of the polycystic kidney disease gene (*PKD1*). *Genomics.* **13:** 35–38.
78. Wienecke, R., A. Konig, and J. E. DeClue. 1995. Identification of tuberin, the tuberous sclerosis-2 product. Tuberin possesses specific Rap1GAP activity. *J. Biol. Chem.* **7:** 16409–16414.
79. Olivecrona, T., S. S. Chernick, G. Bengtsson-Olivecrona, J. R. Paterniti, Jr., W. V. Brown, and R. O. Scow. 1985. Combined lipase deficiency (*cld/cld*) in mice. *J. Biol. Chem.* **260:** 2552–2557.
80. Olivecrona, T., G. Bengtsson-Olivecrona, S. S. Chernick, and R. O. Scow. 1986. Effect of combined lipase deficiency (*cld/cld*) on hepatic and lipoprotein lipase activities in liver and plasma of newborn mice. *Biochim. Biophys. Acta.* **876:** 243–248.
81. Masuno, H., E. J. Blanchette-Mackie, S. S. Chernick, and R. O. Scow. 1990. Synthesis of inactive nonsecretable high mannose-type lipoprotein lipase by cultured brown adipocytes of combined lipase-deficient *cld/cld* mice. *J. Biol. Chem.* **265:** 1628–1638.
82. Davis, R. C., O. Ben-Zeev, D. C. Martin, and M. H. Doolittle. 1990. Combined lipase deficiency in the mouse: evidence of impaired lipase processing and secretion. *J. Biol. Chem.* **265:** 17960–17966.
83. Oka, K., J. G. Yuan, M. Senda, A. S. Masibay, P. K. Oasba, H. Masuno, R. O. Scow, J. R. Paterniti, Jr., and W. V. Brown. 1989. Expression of lipoprotein lipase gene in combined lipase deficiency. *Biochim. Biophys. Acta.* **1008:** 351–354.
84. Oka, K., T. Nakano, G. T. Tkalcevic, R. O. Scow, and W. V. Brown. 1991. Molecular cloning of mouse hepatic triacylglycerol lipase: gene expression in combined lipase-deficient (*cld/cld*) mice. *Biochim. Biophys. Acta.* **1089:** 13–20.
85. Lusis, A. J., B. A. Taylor, D. Quon, S. Zollman, and R. C. LeBoeuf. 1987. Genetic factors controlling structure and expression of apolipoproteins B and E in mice. *J. Biol. Chem.* **262:** 7594–7604.
86. Warden, C. H., R. C. Davis, M-Y. Yoon, D. Y. Hui, K. Svenson, Y-R. Xia, K-Y. He, and A. J. Lusis. 1993. Chromosomal localization of lipolytic enzymes in the mouse: pancreatic lipase, colipase, hormone-sensitive lipase, hepatic lipase, and carboxyl ester lipase. *J. Lipid Res.* **34:** 1451–1455.
87. Eckel, R. H. 1989. Lipoprotein lipase: a multifunctional enzyme relevant to common metabolic diseases. *N. Engl. J. Med.* **320:** 1060–1068.
88. Leitersdorf, E., O. Stein, and Y. Stein. 1984. Synthesis and secretion of triacylglycerol lipase by cultured rat hepatocytes. *Biochim. Biophys. Acta.* **794:** 261–268.
89. Olivecrona, T., S. S. Chernick, G. Bengtsson-Olivecrona, M. M. Garrison, and R. O. Scow. 1987. Synthesis and secretion of lipoprotein lipase in 3T3-L1 adipocytes. *J. Biol. Chem.* **262:** 10748–10759.
90. Masuno, H., C. J. Schultz, J. W. Park, E. J. Blanchette-Mackie, C. Mateo, and R. O. Scow. 1991. Glycosylation, activity and secretion of lipoprotein lipase in cultured brown adipocytes of newborn mice. *Biochem. J.* **277:** 801–809.
91. Amri, E., C. Vannier, J. Etienne, and G. Ailhaud. 1986. Maturation and secretion of lipoprotein lipase in cultured adipose cells. II. Effects of tunicamycin on activation and secretion of the enzyme. *Biochim. Biophys. Acta.* **875:** 334–343.
92. Vannier, C., and G. Ailhaud. 1989. Biosynthesis of lipoprotein lipase in cultured mouse adipocytes. II. Processing, subunit assembly, and intracellular transport. *J. Biol. Chem.* **264:** 13206–13216.
93. Ong, J. M., and P. A. Kern. 1989. The role of glucose and glycosylation in the regulation of lipoprotein lipase synthesis and secretion in rat adipocytes. *J. Biol. Chem.* **264:** 3177–3182.
94. Semenkovich, C. F., C-C. Luo, M. K. Nakanishi, S-H. Chen, L. C. Smith, and L. Chan. 1990. In vitro expression and site-specific mutagenesis of the cloned human lipoprotein lipase gene. *J. Biol. Chem.* **265:** 5429–5433.
95. Wölle, J., H. Jansen, L. C. Smith, and L. Chan. 1993. Functional role of N-linked glycosylation in human hepatic lipase: asparagine-56 is important for both enzyme activity and secretion. *J. Lipid Res.* **34:** 2169–2176.
96. Ben-Zeev, O., G. Stahnke, G. Liu, R. C. Davis, and M. H. Doolittle. 1994. Lipoprotein lipase and hepatic lipase: the role of asparagine-linked glycosylation in the expression of a functional enzyme. *J. Lipid Res.* **35:** 1511–1523.
97. Ben-Zeev, O., M. H. Doolittle, R. C. Davis, J. Elovson, and M. C. Schotz. 1992. Maturation of lipoprotein lipase: expression of full catalytic activity requires glucose trimming but not translocation to the *cis*-Golgi compartment. *J. Biol. Chem.* **267:** 6219–6227.
98. Verhoeven, A. J. M., and H. Jansen. 1990. Secretion of rat hepatic lipase is blocked by inhibition of oligosaccharide processing at the stage of glucosidase I. *J. Lipid Res.* **31:** 1883–1893.
99. Carroll, R., O. Ben-Zeev, M. H. Doolittle, and D. L. Severson. 1992. Activation of lipoprotein lipase in cardiac myocytes by glycosylation requires trimming of glucose residues in the endoplasmic reticulum. *Biochem. J.* **285:** 693–696.
100. Cheng, C. C., and D. Bennett. 1980. Nature of the antigenic determinants of T locus antigens. *Cell.* **19:** 537–543.
101. Hammond, C., I. Braakman, and A. Helenius. 1994. Role of N-linked oligosaccharide recognition, glucose trimming, and calnexin in glycoprotein folding and quality control. *Proc. Natl. Acad. Sci. USA.* **91:** 913–917.
102. Ware, F. E., A. Vassilakos, P. A. Peterson, M. R. Jackson, M. A. Lehrman, and D. B. Williams. 1995. The molecular chaperone calnexin binds $Glc_1Man_9GlcNAc_2$ oligosaccharide as an initial step in recognizing unfolded glycoproteins. *J. Biol. Chem.* **270:** 4697–4704.
103. Jannatipour, M., and L. A. Rokeach. 1995. The *Schizosaccharomyces pombe* homologue of the chaperone calnexin is essential for viability. *J. Biol. Chem.* **270:** 4845–4853.
104. de Silva, A. M., W. E. Balch, and A. Helenius. 1990. Quality control in the endoplasmic reticulum: folding and misfolding of vesicular stomatitis virus G protein in cells and in vitro. *J. Cell Biol.* **111:** 857–866.
105. Gething, M-J., and J. Sambrook. 1992. Protein folding in the cell. *Nature.* **355:** 33–45.
106. Rowling, P. J. E., and R. B. Freedman. 1993. Folding, assembly, and posttranslational modification of proteins within the lumen of the endoplasmic reticulum. *In* Subcellular Biochemistry. Volume 21: Endoplasmic Reticulum. N. Borgese and J. R. Harris, editors. Plenum Press, New York. 41–80.
107. Peterson, J., W. Y. Fujimoto, and J. D. Brunzell. 1992. Human lipoprotein lipase: relationship of activity, hepa-

rin affinity, and conformation as studied with monoclonal antibodies. *J. Lipid Res.* **33:** 1165–1170.

108. Hunt, C. R., D. L. Gasser, D. D. Chaplin, J. C. Pierce, and C. A. Kozak. 1995. Chromosomal localization of five murine HSP70 gene family members: Hsp70-1, Hsp70-2, Hsp70-3, Hsc70t, and Grp78. *Genomics.* **16:** 193–198.
109. Sternlicht, H., G. W. Farr, M. L. Sternlicht, J. K. Driscoll, K. Willison, and M. B. Yaffe. 1993. The *t*-complex polypeptide 1 complex is a chaperonin for tubulin and actin in vivo. *Proc. Natl. Acad. Sci. USA.* **90:** 9422–9426.
110. Noiva, R., and W. J. Lennarz. 1992. Protein disulfide isomerase. A multifunctional protein resident in the lumen of the endoplasmic reticulum. *J. Biol. Chem.* **267:** 3553–3556.
111. Mazzarella, R. A., M. Srinivasan, S. M. Haugejorden, and M. Green. 1990. Erp72, an abundant luminal endoplasmic reticulum protein, contains three copies of the active site sequences of protein disulfide isomerase. *J. Biol. Chem.* **265:** 1094–1101.
112. Haugejorden, S. M., M. Srinivasan, and M. Green. 1991. Analysis of the retention signals of two resident luminal endoplasmic reticulum proteins by in vitro mutagenesis. *J. Biol. Chem.* **266:** 6015–6018.
113. Qu, D., R. A. Mazzarella, and M. Green. 1994. Analysis of the structure and synthesis of GRP94, an abundant stress protein of the endoplasmic reticulum. *DNA Cell Biol.* **13:** 117–124.
114. Schindler, R., C. Itin, M. Zerial, F. Lottspeich, and H-P. Hauri. 1993. ERGIC-53, a membrane protein of the ER-Golgi intermediate compartment, carries an ER retention motif. *Eur. J. Cell Biol.* **61:** 1–9.
115. Willnow, T. E., S. A. Armstrong, R. E. Hammer, and J. Herz. 1995. Functional expression of low density lipoprotein receptor-related protein is controlled by receptor-associated protein in vivo. *Proc. Natl. Acad. Sci. USA.* **92:** 4537–4541.
116. Bu, G., H. J. Geuze, G. J. Strous, and A. L. Schwartz. 1995. 39 kDa receptor-associated protein is an ER resident protein and molecular chaperone for LPL receptor-related protein. *EMBO J.* **14:** 2269–2280.
117. Lisitsyn, N. A., J. A. Segre, K. Kusumi, N. M. Lisitsyn, J. H. Nadeau, W. N. Frankel, M. H. Wigler, and E. S. Lander. 1994. Direct isolation of polymorphic markers linked to a trait by genetically directed representational difference analysis. *Nat. Genet.* **6:** 57–63.
118. Doolittle, M. H., H. Wong, R. C. Davis, and M. C. Schotz. 1987. Synthesis of hepatic lipase in liver and extra-hepatic tissues. *J. Lipid Res.* **28:** 1326–1334.
119. Artzt, K., P. McCormick, and D. Bennet. 1982. Gene mapping within the *T/t* complex of the mouse. I. *t*-Lethal genes are nonallelic. *Cell.* **28:** 463–470.
120. Dunn, L. C., D. Bennet, and J. Cookingham. 1973. Polymorphisms for *t*-lethals in European populations of *Mus musculus*. *J. Mammal.* **54:** 822–830.